

Grassland Obligates and Declining Birds Operate Near Edges of Body Mass Distributions

Introduction

Much of the world's native grassland habitat has been lost in recent decades to agricultural and other anthropogenic land use conversion [1]. The conversion of native grassland to row crops which are increasingly subjected to intensified agricultural practices, have resulted in biodiversity loss which are easily measured by examining long-term changes in bird populations and communities. Native grasslands not converted for agricultural practice or other development are still subject to change due to changes in the feedbacks regulating native grass production, including a loss of wild and prescribed fire and woody plant encroachment [2, 3, 4]. Understanding whether these changes manifest in terrestrial communities is an important step towards understanding if, where, and how conservation efforts may be made to protect these areas.

Animal body mass distributions have been used to identify scaling structures of ecological communities [5, 6, 7]. Using statistical methods to identify gaps, or discontinuities, in body mass distributions, some patterns are observed within and across taxonomic groups and biomes. Given the ubiquity of discontinuities identified in body mass distributions of fauna and social systems [8], the ecological significance of these patterns may prove useful in understanding ecosystem structure and functioning [9]. Various hypotheses are postulated as drivers of the observed discontinuities in animal body mass distributions, including those related to resource use (the Energetic and Textural Discontinuity hypotheses), community interactions, biogeography, and evolution/phylogenetics [5, 7, 10, 11, 12].

Body size influences the frequency and intensity of inter- and intraspecific competition for resources, territory, and mates, thereby dictating the spatial and temporal scales at which a species of a distinct body size operates [13, 14, 15]. The scaling structure of terrestrial communities have been found to have 'lumpy' distributions; that is, they are not well-described using parametric statistical descriptions. If the scaling structure of a community manifests in the body mass distribution of the community, it is considered reflective of the discontinuous and heterogeneous nature of resource use. Specifically, [7] suggests that the body mass distribution of a community or group of species reflects the discontinuous nature of environmental structures and processes. Quantitative analyses of animal body sizes [16, 17] and other similar distributions has revealed the ubiquity of the discontinuous nature of distributions of animal body masses [18, 19], plant biomass [20], city population sizes [21], and animal home range sizes [22].

A recent study of the Central United States, including and beyond the Great Plains ecoregions, used discontinuity analysis of body mass distributions to identify the locations of what they refer to as 'spatial regimes' over an approximately 50 year period [23]. The authors concluded that a spatial regime boundary exists in this region, and has been moving poleward as a consequence of large-scale drivers including woody plant encroachment, fire suppression, and climate change. Using the boundaries identified in this study I seek to determine whether this 'shifting spatial regime' manifests in the grasslands of the Central Great Plains.

Avian distribution and presence data are abundant, easily accessible and, more importantly, provide insights into resource availability and structure at the local and landscape scales. In this Chapter, I first use discontinuity analysis of avian body mass distributions to identify the scaling structures of local avian communities in the Prairie Potholes, Central Mixed Grass, and Eastern Tall Grass regions of the central Great Plains of North America. I then use these distributions to determine whether the shifting spatial regime proposed by [23] manifests in the grassland bird community which is most susceptible to native grassland habitat loss or degradation [24]. Although I find no evidence to support the hypothesis of the spatial regime boundary suggested in [23], the results from this study support previous hypotheses that vulnerable species operate at the 'edge' of body mass aggregations.

Methods

Study area

A recent study [roberts2019shifting] identified what they refer to as spatial regimes across a large portion of the central United States [see Figure @ref(fig:studyArea)]. The authors hypothesize that a spatial regime boundary exists in the Central Great Plains and suggests it has exhibited a Northward shift at a rate of $\sim \frac{0.05^\circ \text{ latitude}}{\text{year}}$. The authors used discontinuity analysis to identify these ‘spatial regimes’, using the body mass of breeding bird communities. Their hypothesized spatial regime boundary occurs at 39° latitude in year 1970, 39.5° latitude in year 1985, 40° latitude in year 2000, and 40.5° latitude in year 2015 (see Figure @ref(fig:routesWithSpatRegimes)). Sampling sites were classified each year as belonging to either the Southern or Northern regime according to whether the location was below (Southern) or above (Northern) the regimes identified by roberts2019shifting.

The study area is designed such that there is minimal crossing of very different BCR, or habitat types (Figure @ref(fig:studyarea)). In other words, this study area largely falls within BCRs which can be generally classified as grassland habitat (BCR 11, Prairie Potholes; BCR 19, Central Mixed Grass ; BCR 22, Eastern Tall Grass). Using this design we should expect that the functional groups within our avian communities should be similar across BCR boundaries, despite a potential turnover in species identity. Accounting for change in habitat across space allows us to assume that any observed change in the scaling structure of the avian community is due to changes in habitat and resource availability such that similar species are or are not included in the community.

Data

Avian census data - North American Breeding Bird Survey

I constructed body mass distributions using route-level data from the North American Breeding Bird Survey hereafter [NABBS; @bbsData]. The NABBS uses citizen scientist volunteers to annually collect data using a standardized roadside, single observer, 3-minute point count protocol and has organized data collection annually across North America (Figure @ref(fig:bbsPoints)) since 1966. Each roadside survey consists of 50, 3-minute point counts (data collected using sight and sound) along ~ 24.5 mile stretch of road. Although the point counts are designed to collect estimates of relative abundance, the method for building body mass distributions used in this chapter require only presence absence data. I therefore converted abundances to presence-absence data. I considered a species as ‘present’ if it was detected on the year in question or the ± 1 year to account for potential false negative observations (i.e., a species was not detected in the NABBS route despite its presence in the local community).

Identifying avian census locations

To determine whether the spatial regime shifts identified in roberts2019shifting manifested in local avian community structure, I restricted analysis to the grassland habitat of the Central Great Plains. All routes falling within a rectangular area bounded by coordinates 37.8° and 44.5° latitude, and -101° and -95.5° longitude [see Figure @ref(fig:routesWithSpatRegimes)]. I retained all NABBS routes which used the sampling protocol ‘101’, which is the standard method for conducting NABBS point count surveys.

Avian body mass data

Species operating at similar spatial and temporal scales are those which are close in body size as identified using statistical aggregation identification techniques [allen_body_1999; Section @ref(discontAnaly)]. The interactions among species within a single body mass aggregation are presumed to experience a higher frequency and intensity of interspecific interactions with each other as opposed to those in different aggregations [peterson1998ecological]. Although some species of birds are sexually size dimorphic, I am unaware of any sexually size-dimorphic birds that would likely operate at different spatial and temporal. Therefore, I constructed body mass distributions of each avian census using the sex-averaged body masses published in @dunning2007crc (available for download at CRC press).

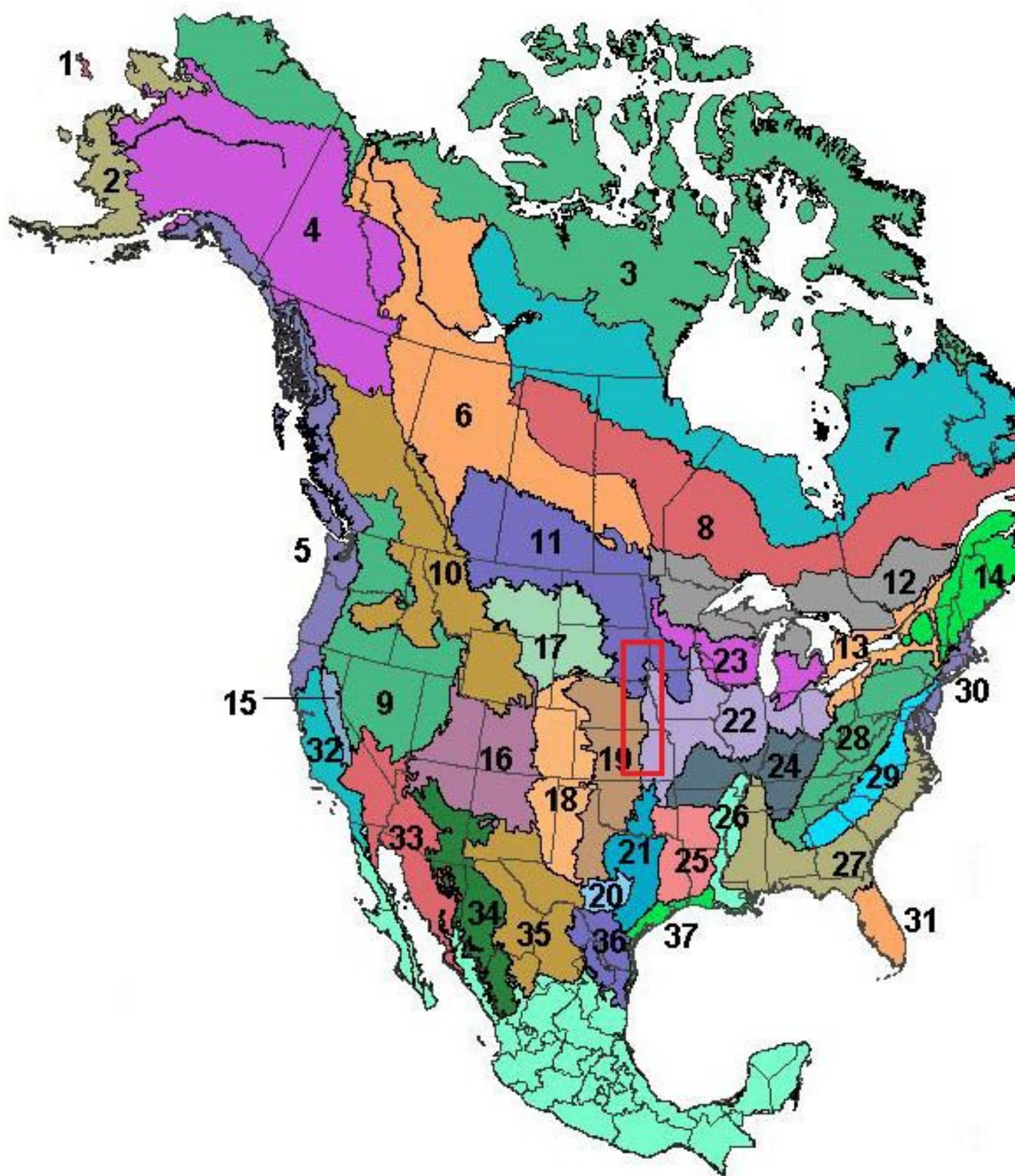


Figure 1: My study area (red box) overlaying the terrestrial Breeding Conservation Regions (BCR) in North America.

Removing species from analysis

Due to strict reliance on volunteers, some routes are not covered every year. Although NABBS volunteers attempt identify all species in the point-count area, biases exist in data collection. Rather than retain observations of cryptic or species with low detection rates, I removed select species from the censuses (see Methods section in Chapter @ref(fisherSpatial) for further discussion of this topic). I analyzed species of the following taxonomic families: Accipitriformes, Apodiformes, Cathartiformes, Charadriiformes, Columbiformes, Coraciiformes, Cuculiformes, Galliformes, Gruiformes, Passeriformes and Piciformes. Although removing cryptic, nocturnal, and some crepuscular species (e.g. Caprimulgiformes) from the analysis may yield a more conservative body mass distribution, including them may result in correctly identifying additional scaling structures (or body mass aggregations) in some routes but not in others. This method of exclusion also results in a loss of some medium- and larger-bodied Ciconiiformes (Podicipediformes, Phoenicopteriformes, Ciconiiformes; e.g. grebes, pelicans).

Taxonomic munging of the census data

Although the NABBS survey reports species-specific abundances, some birds are only classified to genera or order. Common examples of these species are those which are nearly indistinguishable from each other (e.g., Glossy Ibis and White-faced Ibis), birds which are difficult to see under certain conditions (e.g., hummingbirds, fast-moving hawks or accipiters), or species whose songs are similar. Numerous species were presented as identified to family or genus (e.g., Accipiter sp., Buteo sp., and Trochilids sp.) and others are categorized as hybrid.

I made decisions regarding species-specific classification based on the North American breeding range maps provided by the Cornell Lab of Ornithology. Many unidentified species were easily categorized given the lack of overlap in species' ranges in our study area. For example, *Baeolophus bicolor* is nearly indistinguishable from *Baeolophus atricristatus*, however *B. atricristatus* is not known to occur in our study area (Figure @ref(fig:studyarea))—therefore all accounts classified as either *B. bicolor* or *B. atricristatus* were classified as the former. This example occurred for. Informed decisions like of this nature were made regarding the following unidentified species, where the second name in the binomial was assigned as the species preceding the “/”: *Passerina cyanea* / *amoena*, *Corvus brachyrhynchos* / *ossifragus*, *Petrochelidon pyrrhonota* / *fulva*, *Corvus brachyrhynchos*, *Quiscalus major* / *mexicanus*, *Pipilo maculatus* / *erythrophthalmus*, *Sturnella magna* / *neglect*, *Plegadis chihi* / *falcinellus*, *Coccyzus erythrophthalmus* / *americanus*, *Empidonax traillii* / *alnorum*, *Icterus galbula* / *bullockii*, *Nyctanassa nycticorax* / *violacea*, and *Poecile atricapillus* / *carolinensis* were all classified according to their known distributions. I classified unidentified hummingbirds (*Trochilid* sp.) as *Selasphorus rufus*, and unidentified Terns (Tern sp.) as *Chlidonias niger*. All unidentified Accipiters (Accipiter sp.), Buteos (Buteo sp.), and Gulls (Gull sp.) were removed from analysis entirely as there are no clear differences in the probability of occurrence in our study area.

Identifying species of interest

@allen2006body propose alternative hypotheses for the relative locations of species within the body mass aggregation distributions as a function of ‘distance-to-edge’, a measure indicating the distance (in log-mass units) of each species to the edge of a body mass aggregation (methods described in Section @ref(discontAnaly)). This distance-to-edge measure is zero when the species falls at the edge of a statistically identified body mass aggregation. This species is often referred to as an ‘edge species’. To determine the effect of spatial regime shifts on edge species, I identified three types of species of interest: (1) grassland obligates species, (2) species with widespread population declines in the study area, and (3) a combination of these groups. All remaining species were classified as ‘other’.

Grassland obligate species

The spatial regimes identified in @roberts2019shifting are attributed to large-scale changes in the landscape, including woody plant invasion. The loss of native grassland in our study area due to land conversion is largely attributed to anthropogenic land use change (e.g., development) and fire suppression. Numerous species have been negatively impacted by this widespread habitat loss, but grassland obligates are particularly

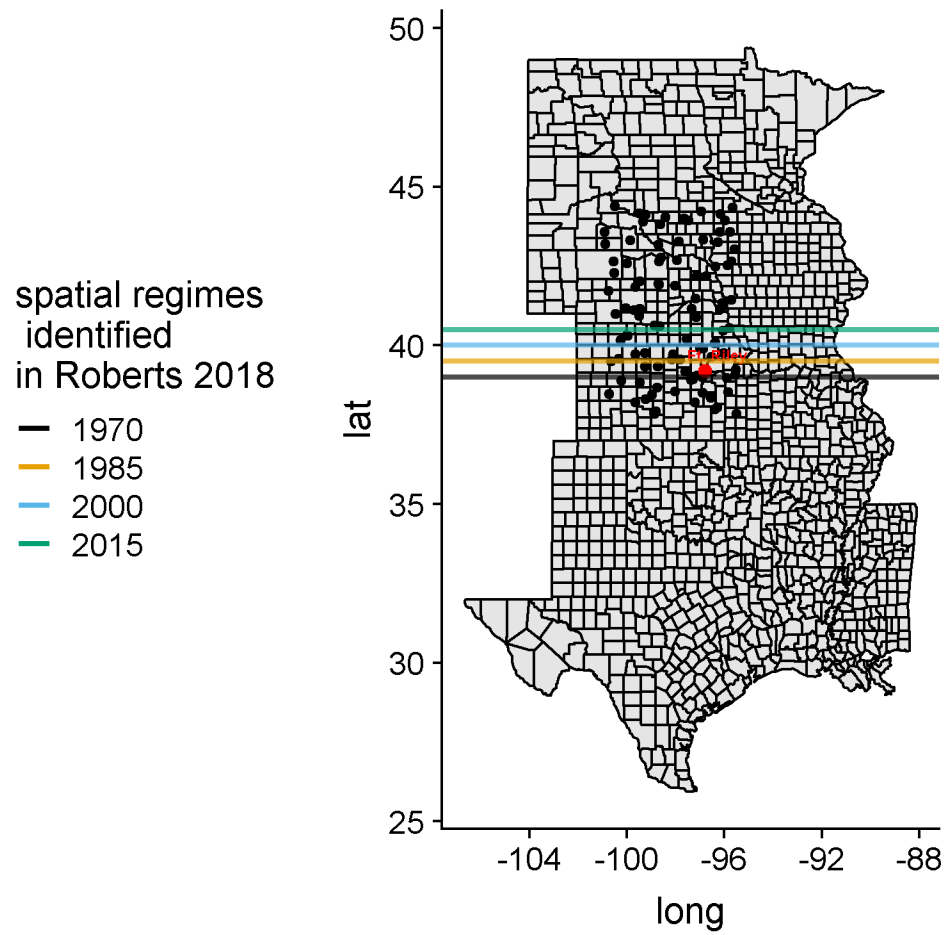


Figure 2: North American Breeding Bird Survey routes (points), latitudinal locations (horizontal bars) of the spatial regimes identified by @roberts2019shifting.

at risk. Grassland obligates should be strong indicators of the large-scale spatial regime shifts identified in @roberts2019shifting, given their high sensitivity to grassland habitat loss [@herkert1994effects]. I identified North American grassland obligate species from the grey literature [@shriner2005distribution; @north2009state] and white literatures [@peterjohn1999population]. Although some grassland obligates were positively impacted by the Conservation Reserve Program [CRP; @peterjohn1999population], this group of birds exhibited strong declines in North America until approximately 2003, the year the Farm Bill was adopted [@north2009state].

Declining species

I classified a species as ‘declining’ based on the results of the North American Breeding Bird Survey [@sauer2017results]. The Patuxent Wildlife Research Center uses hierarchical modelling techniques to estimate the trends of species using the NABBS data at various spatial scales. @sauer2017results also provides estimates of data credibility according to data availability, number of routes used to build the population trend estimate, abundance, and probability of detecting a small change in population trend. These credibility scores are generated for multiple spatial extents: state-level, BCR-level, and across the three regions of the United States (Western, Central, and Eastern). Given the extent of this study, I considered the data credibility estimates using the Central Breeding Bird Survey Region, the Prairie Pothole BCR (BCR 11) and Eastern Tallgrass Prairie (BCR 22). A species was considered as declining only if the trend estimate was categorized as having moderate precision and abundance (blue) or having a deficiency (yellow). I considered the population trend estimates provided for the period of 1966 - 2015.

Statistical analysis

Identifying scaling structure of avian communities using body mass distributions

Discontinuities in body mass distributions been quantified using various methods (e.g., multivariate time series models, regression trees, and gap rarity index) which are collectively referred to as ‘discontinuity analyses’ [@nash2014discontinuities; @barichievy2018method; @stow2007evaluating; @allen2009discontinuities]. Using various methods, the discontinuous nature of body masses of ecological communities is well-documented, having been observed in various taxa of both terrestrial [@allen2006patterns] and aquatic [@spanbauer2016body] communities. Multiple methods are proposed for identifying discontinuities in body mass aggregations [@allen2001cross], including clustering algorithms [@stow2007evaluating], body mass difference indices [@holling1992cross], gap rarity index [@restrpo], and more recently the discontinuity detector [@barichievy2018method], an extension of the gap rarity index [@restrepo2008discontinuities].

I used the discontinuity detector described in @barichievy2018method, which uses likelihood to determine whether the observed data contains multiple modes as compared to that of a Gaussian (unimodal) distribution. This method requires multiple user-defined parameters, including an imputation resolution (1000) and a bootstrap sample size (1000) over which the null distribution is randomly sampled. I provided a slightly altered and annotated version of the functions `Neutral.Null` and `Bootstrap.Gaps` (first printed in @barichievy2018method) used to identify discontinuities in a continuous variable in Appendix @ref(appDiscont).

Two criterion have been used to determining the exact location of discontinuities within a rank-ordered continuous variable: using a constant significance/threshold level [@barichievy2018method] and a power constant table for varying sample sizes [@roberts2019shifting]. It should be noted because the power-constant method identifies a larger proportion of “significant” discontinuities, or edges, identifying aggregations requires subjective measures regarding actual aggregation locations. Using the percentile method avoids this subjectivity, however, the aggregation number and locations are sensitive to choice of percentile or threshold value. Following the methods of @barichievy2018method I considered a value to be a discontinuity if the gap percentile (see Appendix @ref(appDiscont)) was ≥ 90 .

I built route-level body mass distributions for each route-year combination by using presence absence data from the current, previous, and following year to account for observational and process errors impacting the detectability of a species within a single route. Using this method reduces the amount of species-specific, and consequently specific-body mass turnover within a route over time. This also assumes that an unobserved

species is truly absent, an assumption which is difficult to avoid without a sophisticated occupancy modelling approach for each species in the community.

Determining Effects of a Spatial Regime Boundary on Grassland Birds

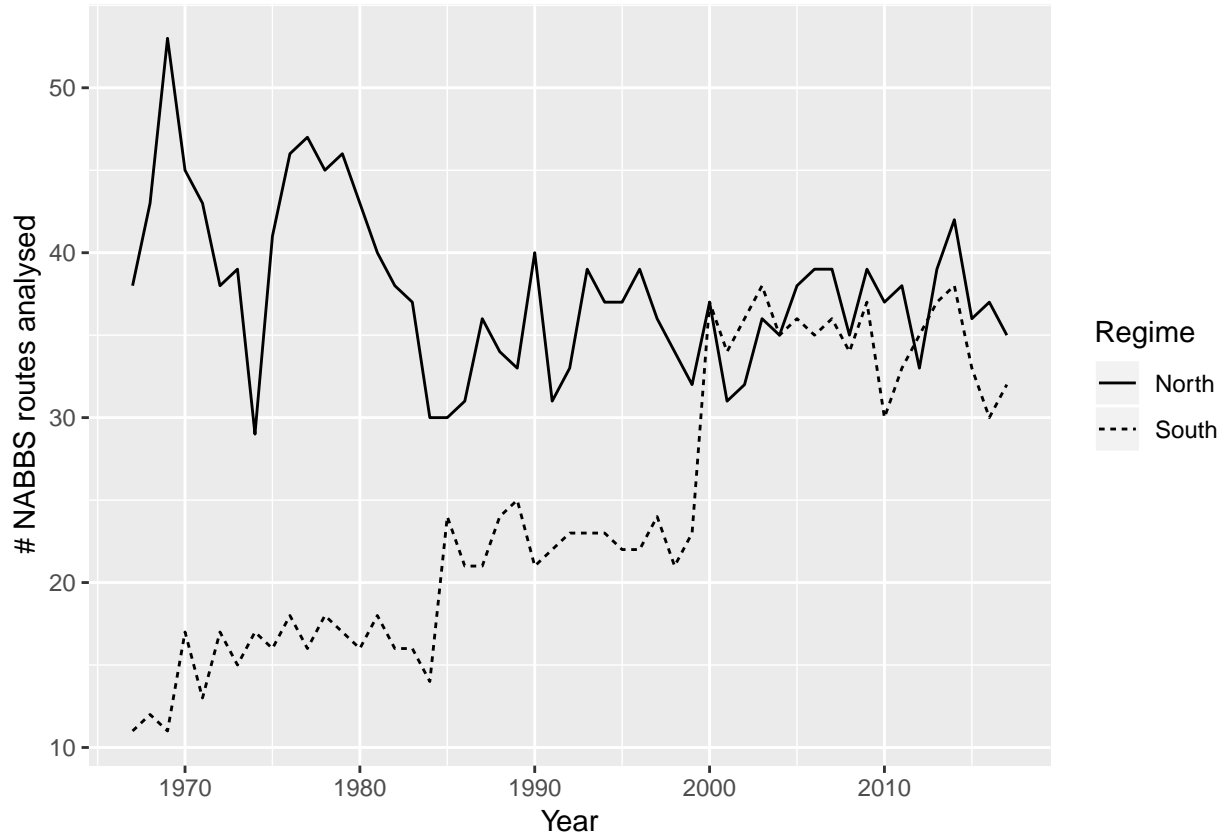
If the spatial regime shift occurred in the bird community, it should manifest in the local community scaling structure through one or both of species turnover and a shift in the number of body mass aggregations. I used linear mixed modelling to determine whether the local scaling structure and the location of grassland obligates and declining species within these scaling structures are impacted by the spatial regime boundaries proposed by @roberts2019shifting.

I used a linear mixed model to determine whether the proposed moving spatial regime boundaries influenced the location of species of interest (grassland obligates, declining species) within their respective body mass aggregation. Each species was assigned a ‘distance to edge’, which served as a proxy of the proximity of a species to the nearest edge of its respective body mass aggregation. Previous studies suggest that this distance to edge measure can be used to identify zones of transitions, as invasive and threatened species tend to be located at the edges of aggregations [@allen1999body]. Following this hypothesis, one should expect to see changes in the locations of sensitive and declining species change in the areas undergoing so called spatial-regime shift zones [@roberts2019shifting].

I therefore modelled the distance to edge of each species within each NABBS route as a function of time, the regime location [South or North of the boundaries proposed in @roberts2019shifting; see Figure @ref(fig:routesWithSpatRegimes)], and the species group (grassland obligate, declining, declining grassland obligate, other). Although distance to edge was not strongly correlated with body mass (Figure @ref(fig:aggEdgeCorrPlot)), I scaled and centered the response variable (distance to edge; Y_i , where i = year), to avoid predictions beyond zero for the unscaled response. Fixed effects included an interaction among year (β_{1i}) and regime location (β_{2i}), and an interaction among regime (β_{2i}) and species group (β_3). Random intercepts were estimated for each species (b_1) within each NABBS route (b_2). That is, species was nested within route. An autoregressive lag-1 correlation structure was assumed for the random intercept estimates. The model was fitted using restricted maximum likelihood. The model was fitted using `nlme::lme` and was coded as `> nlme::lme(> distEdge.scaled ~ year.centerregime + regimesppGroup, > random = ~ 1 | loc/aou, > correlation = corAR1(form = ~ 1 | loc / aou), > data = dat, > method = "REML")`

Results

Summary statistics of censuses (NABBS data)



Given the location of the study area (Figure @ref(fig:studyarea)) with respect to the location of the contiguous Central Great Plains, fewer NABBS routes falling into the Southern regime were analysed than those in the Northern (Table @ref(tab:nRtesPerRegimePerYearTab), Figure @ref(fig:nRtesPerRegimePerYearTab)). Likely due to the increase in the total number of routes surveyed over time across the entire North American Breeding Bird Survey region, species richness increased over time within our study area (Figure @ref(fig:richnessByYear)). Annual turnover rates were relatively low but became more dispersed over time (Figure @ref(fig:turnoverByYear); Table @ref(tab:richTurnTab)).

Species of interest

A total of 163 species were considered for analysis across the entire study area. 18 were classified as grassland obligate species, or species deemed highly sensitive to changes in amount and quality of grassland habitat. Of the grassland obligates, 13 were considered as declining species. An additional 49 species were classified as non-grassland obligate and declining (Table @ref(tab:sppIntTab)).

The total (Figure @ref(fig:stopTotalSum)) and mean (Figure @ref(fig:stopTotalMean)) number of birds counted within each species group was relatively constant across time in the Prairie Potholes and Eastern Tallgrass Prairie bird conservation regions, but fluctuation in stop totals appeared greater in the Badlands and Prairies BCR (Figures @ref(fig:stopTotalMean), @ref(fig:stopTotalSum)). The latter BCR comprises a much smaller portion of the study area (Figure @ref(fig:studyarea)) and accordingly the coefficient of variation (CV; ratio of deviation to the mean) around the stop totals (Figure @ref(fig:stopTotalCV)) was highest in this region. It is worth noting the high CV (CV is considered low when $< \sim 40$) in all regions.

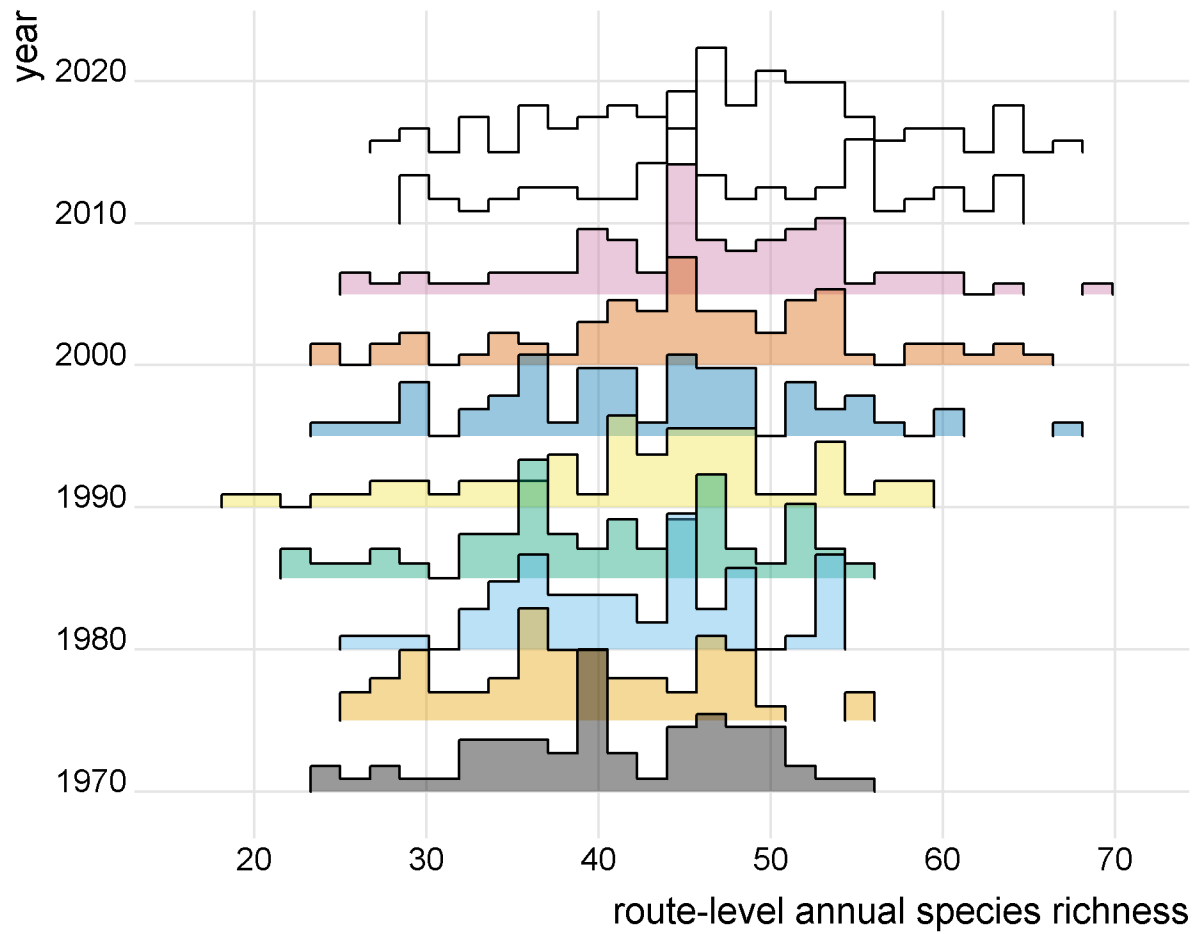


Figure 3: Species richness increases over time across the entire study area.

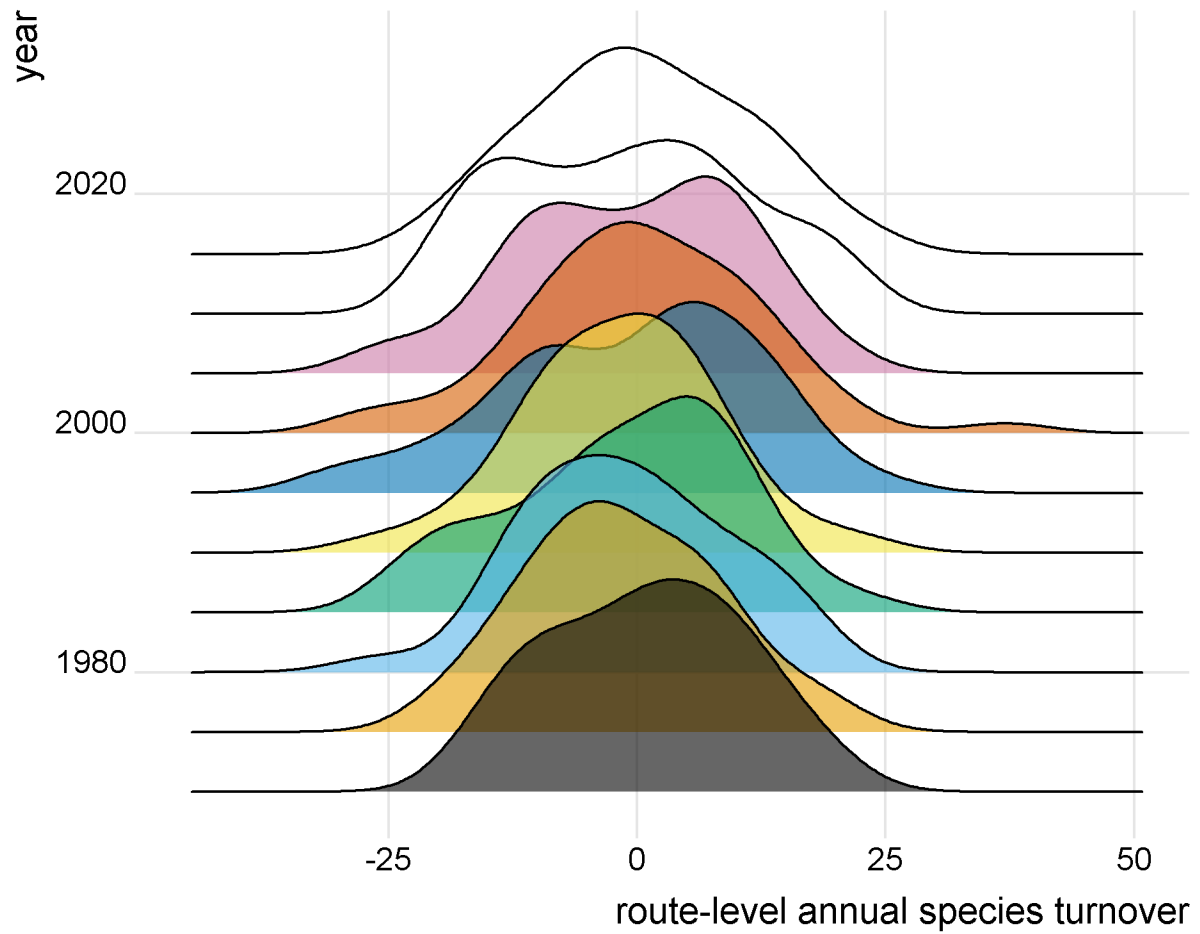


Figure 4: Variance in species turnover increases over time across the entire study area.

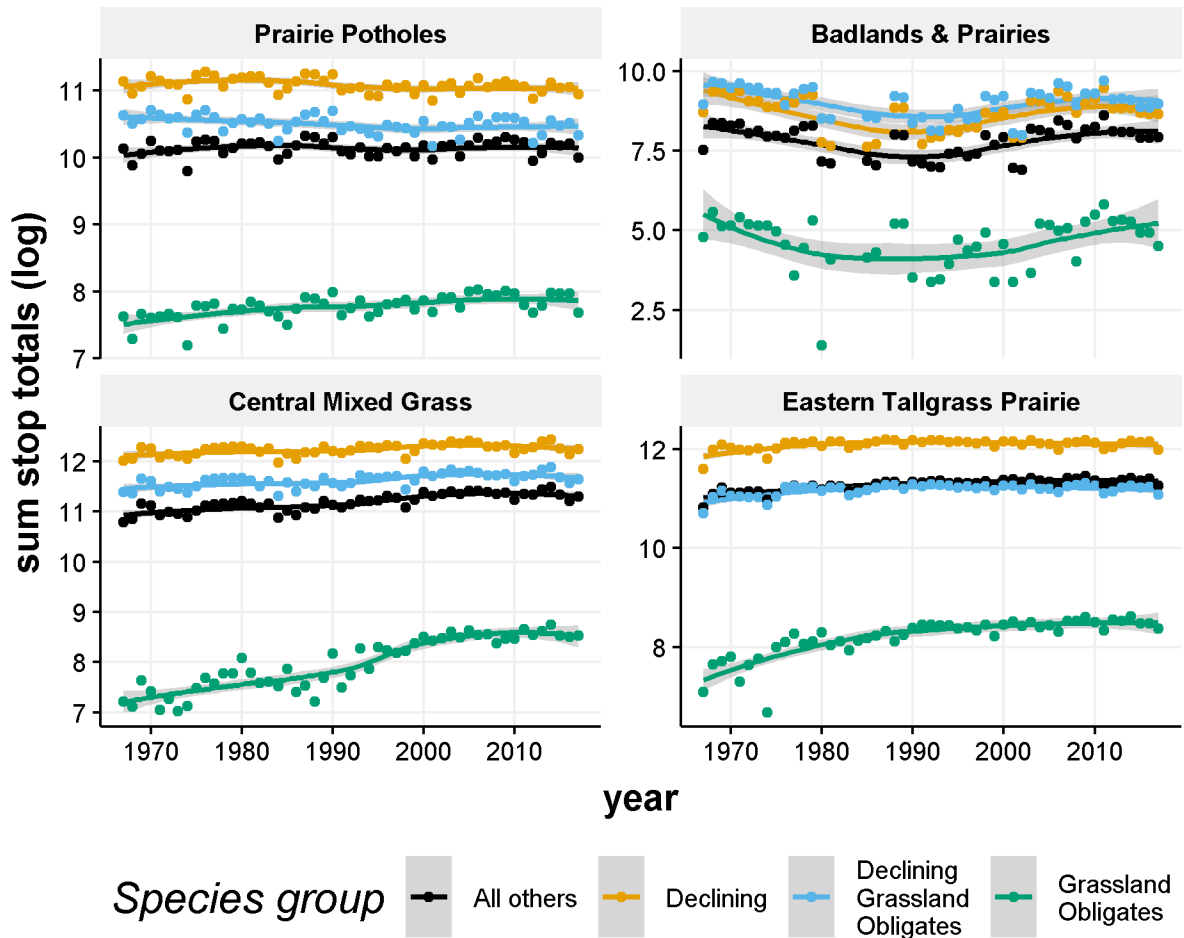


Figure 5: Total number of birds across the entire study area per species group per year.

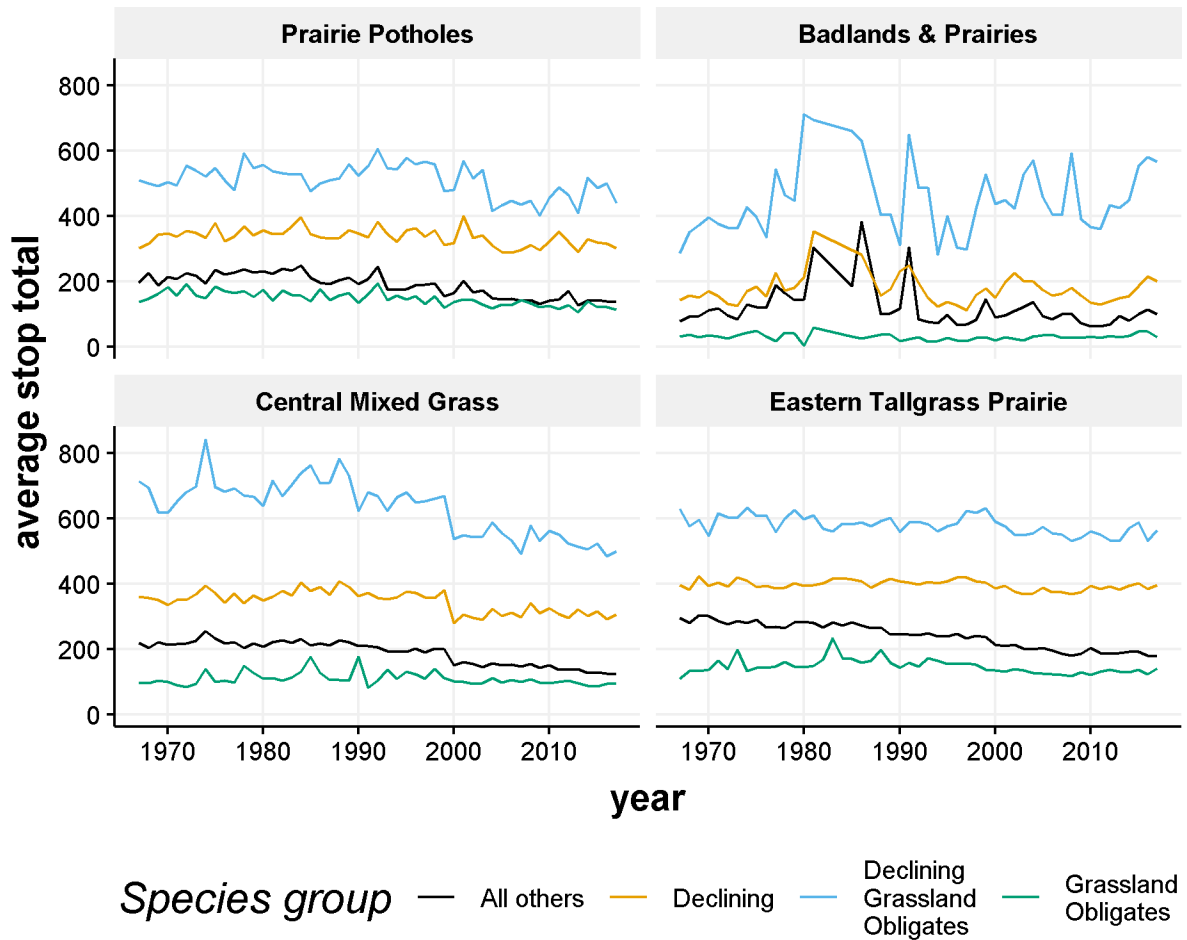


Figure 6: Average number of birds across the entire study area per species group per year.

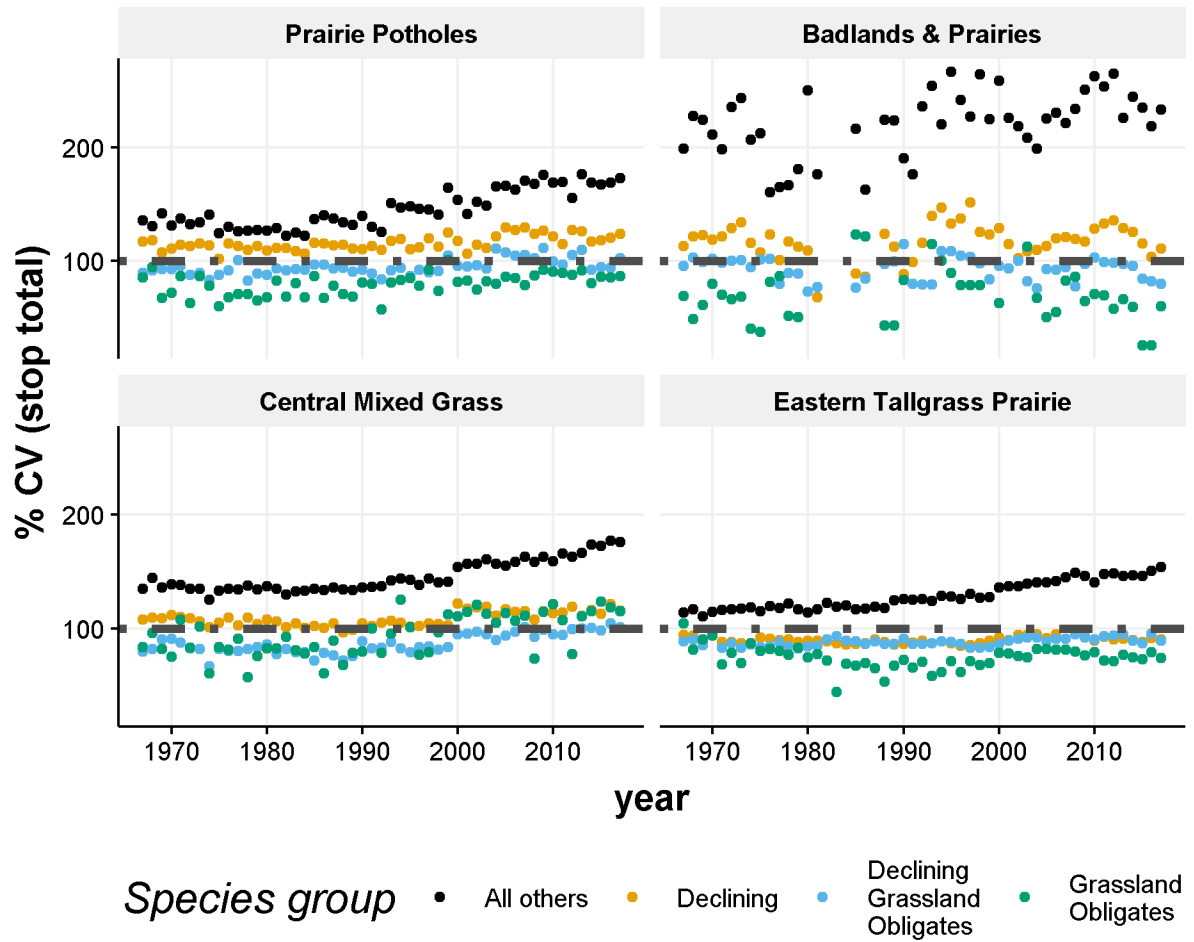


Figure 7: Average number of birds across the entire study area per species group per year.

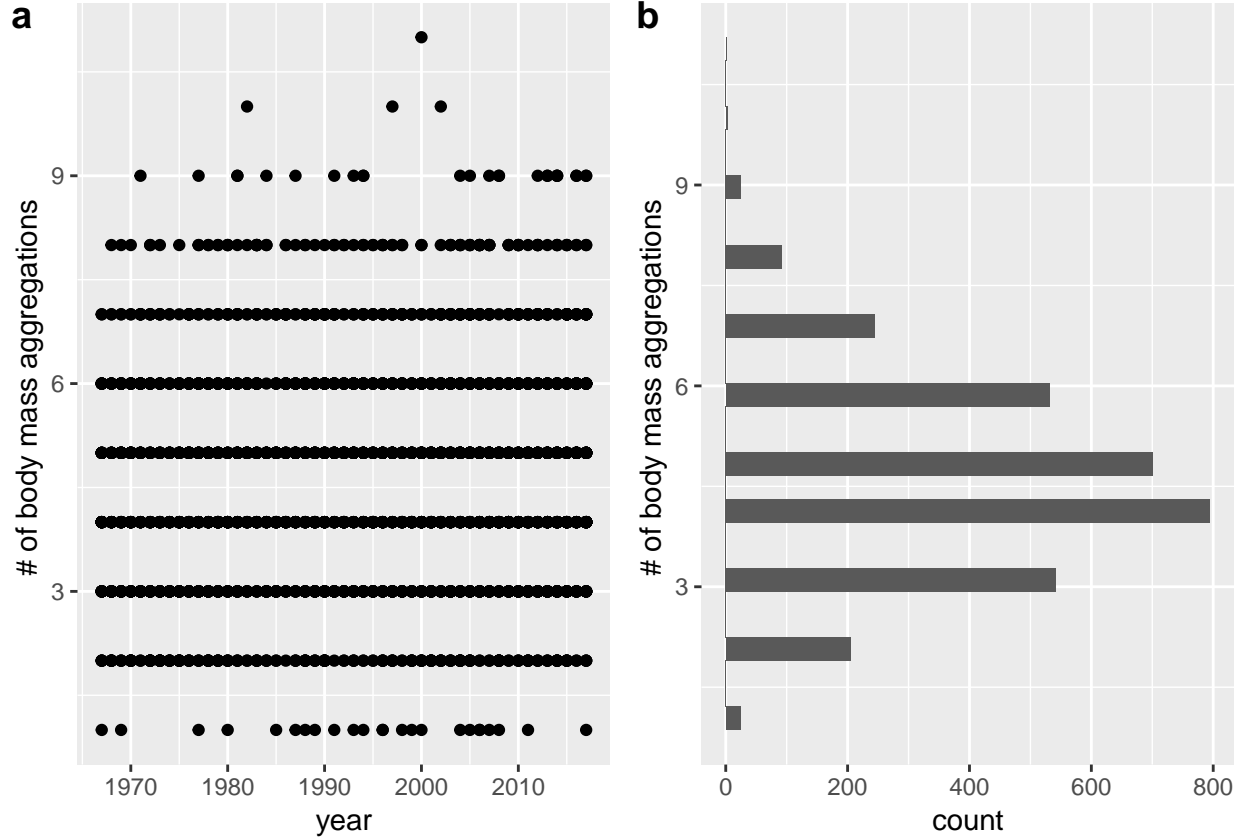


Figure 8: Number of body mass aggregations identified in each route unchanged across the time period (a) and is approximately normally distributed ($\bar{x} = 4.7, \sigma = 1.6$)

Statistical Analysis

Identifying scaling structure in body mass distributions

Discontinuity analysis was conducted to identify the aggregations in the body mass distributions of 103 routes over a 50 period across the Central Great Plains (Figure @ref(fig:studyarea))). Discontinuity analysis suggested discontinuities existed in all routes analysed, and were relatively similar within NABBS routes over time. The number of body mass aggregations identified within each NABBS route using the discontinuity detector [@barichievy2018method] was similar across time (Figure @ref(fig:nAggsPerYear)a) and was approximately normally distributed across all survey-year combinations ($\bar{x} = 4.7, \sigma = 1.6$; Figure @ref(fig:nAggsPerYear)a). Species richness at the route level was strongly positively correlated with the number of aggregations (Figure @ref(fig:aggEdgeCorrPlot)). The distance to edge variable was statistically, but not strongly, correlated with body mass $r = -0.02, p = < 0.01$, and this relationship was similar across species groups (Table @ref(tab:corTabBySppGroup)).

\begin{table}[t]

\caption{Pearson's product correlation coefficient estimate ($r \pm$ lower and upper 95% confidence intervals) of distance-to-edge and body mass (log scale) for all species, grassland obligates, declining species, and declining grassland obligates. }

Species Group	r	\$p\$	df
Grassland Obligates	-0.08(-0.09, -0.07)	0.00	24584
Declining Species	0(-0.01, 0.01)	0.82	86670
Declining Grassland Obligates	-0.09(-0.11, -0.08)	0.00	20519
All Species	-0.02(-0.02, -0.01)	0.00	137946

\end{table}

The discontinuities in the body mass distribution identified appeared relatively similar over time at most NABBS routes (Figure @ref(fig:routeGapEx)). If the shifting spatial regimes proposed in an earlier study [roberts2019shifting; Figure @ref(fig:routesWithSpatRegimes)], then we should expect changes in the body mass distribution of NABBS falling within or near the regime boundary. This was not observed on the routes falling within this zone (Figure @ref(fig:routeGapEx) is representative of the ~5 NABBS locations falling in this area of expected changes shifting).

	Estimate	95% CI
(Intercept)	0.04	(0.02, 0.07)
Year	0.00	(0, 0)
North	0.01	(-0.01, 0.03)
Declining	-0.05	(-0.08, -0.02)
Declining Grassland Obligates	-0.17	(-0.2, -0.14)
Grassland Obligates	0.15	(0.11, 0.2)
Year x Declining	0.00	(0, 0)
North x Declining	0.02	(-0.01, 0.04)
North x Declining Grassland Obligates	-0.05	(-0.07, -0.03)
North x Grassland Obligates	0.04	(0.01, 0.07)

Linear Mixed Effects Analysis of Distance to Edge

Declining species and declining grassland obligate species were located closer to the edge than the ‘other’ species, while grassland obligate species were further from the edge than ‘other’ species (Table @ref(tab:lmeTab)). Similar trends held for declining grassland obligates and grassland obligates in the Northern regime location. There was, however, no evidence to suggest additive effects of the regime location or year, or their interactions (Table @ref(tab:lmeTab)). The lack of additive effects but the presence of multiplicative effects of the regime location (Table @ref(tab:lmeTab)) strengthens the support for the differences in grassland obligates and declining grassland obligates with respect to all other species, however, the confidence intervals around the estimates of declining grassland obligates, grassland obligates suggests the evidence for such an effect is relatively weak.

This is unsurprising given the distribution of grassland obligate body masses is highly skewed right relative to the remaining species (Figures @ref(fig:bmDistPerSppGroup)), @ref(fig:bmDistPerSppGroup-byRegime))). Many grassland obligate species have small body masses, reducing the probability that they will appear in different body mass aggregations, however, depending on the local bird community identities, local grassland obligates may all have similar body masses, removing this effect. The larger, non-declining grassland obligates occur in a relatively small portion of our study area, Shortgrass Prairie BCR (Figures @ref(fig:studyarea),@ref(fig:bmDistPerSppGroup-byBCR)).

Discussion

South-North shifts in the past 50 years have been demonstrated in large scale processes, including bird populations and ranges [sorte2007poleward] and plant hardening zones [mckenney2014change]. The concept of spatial regimes has recently been introduced as a way of describing or identifying large-scale shifts of this nature [roberts2019shifting; sundstrom2017detecting]. The methods and ecological significance of

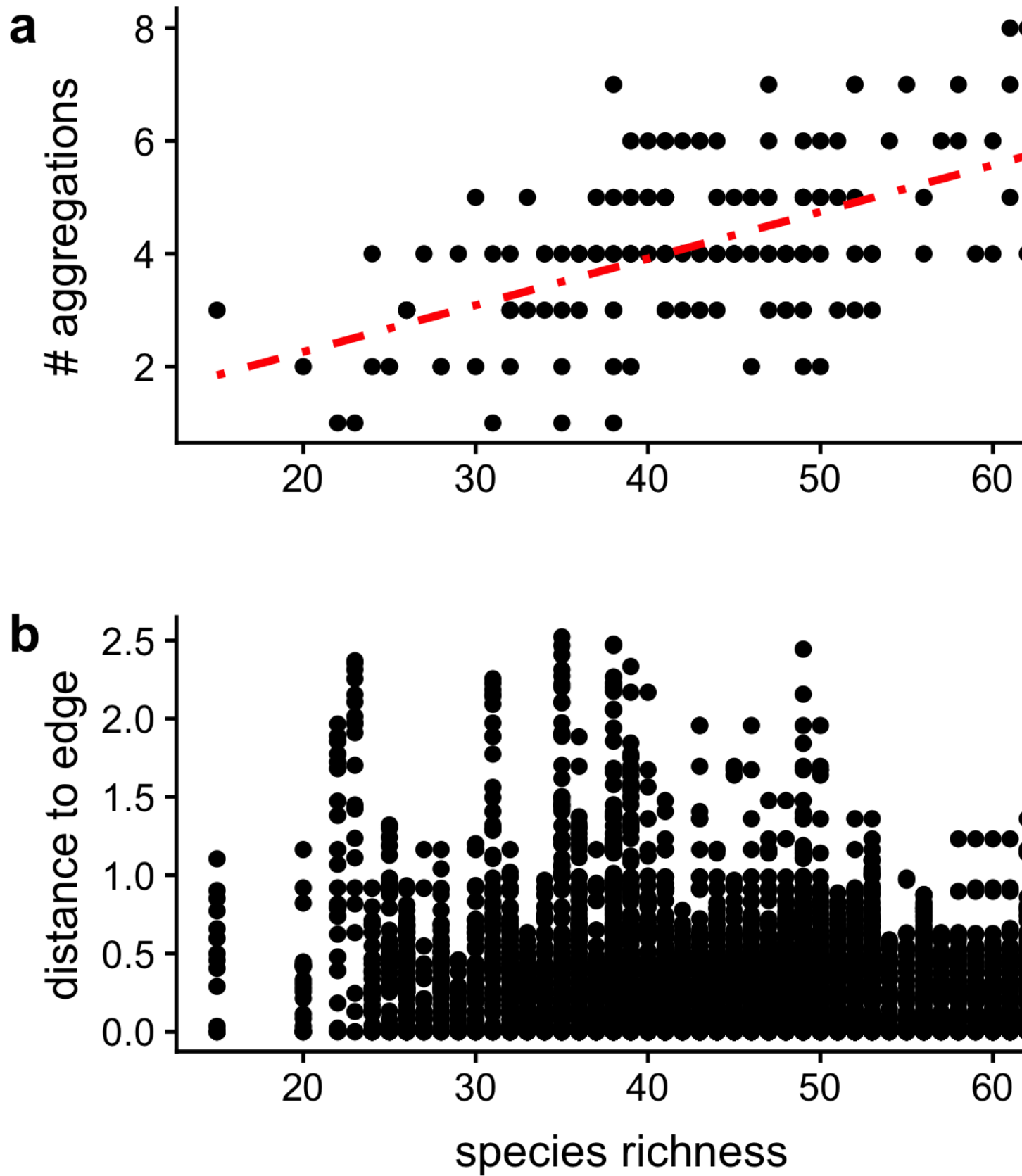
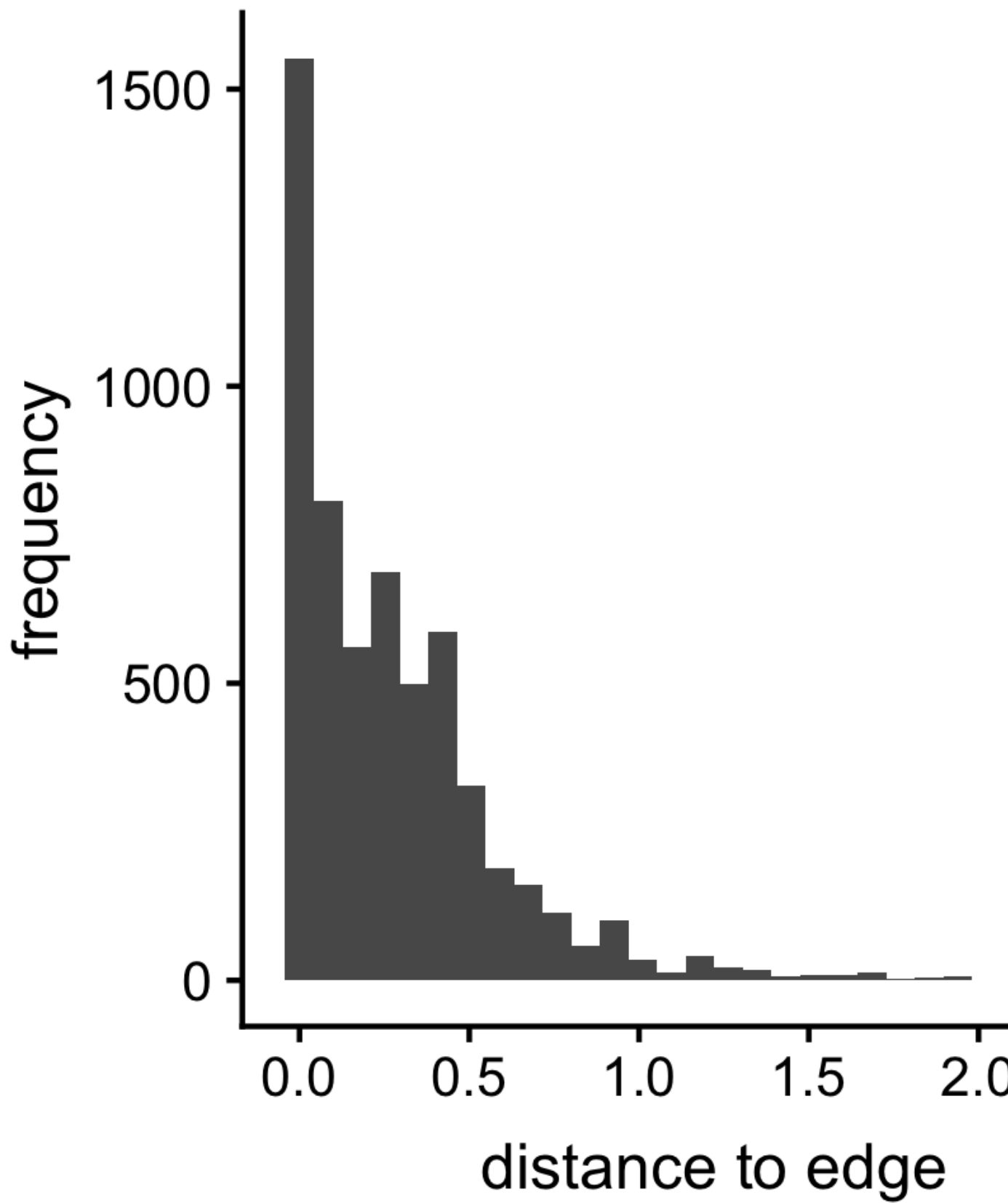


Figure 9: Relationship between species richness per route and (a) the number of aggregations identified in body mass distributions and (b) distance to the edge (units log body mass) of aggregations.



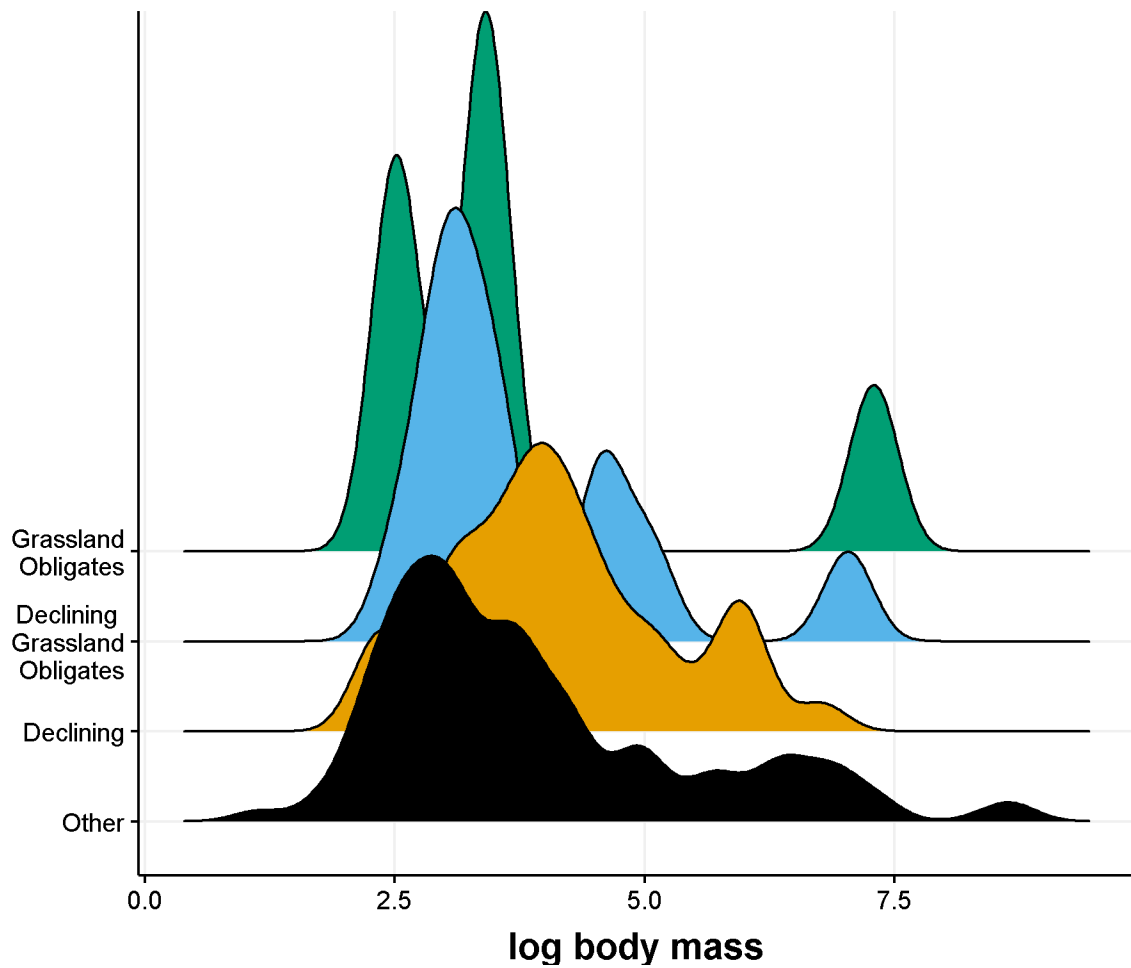


Figure 10: Body mass distribution for species in the study area over the entire time period varies by species group. Distributions represent the species pool for each group over the entire study area and all years.

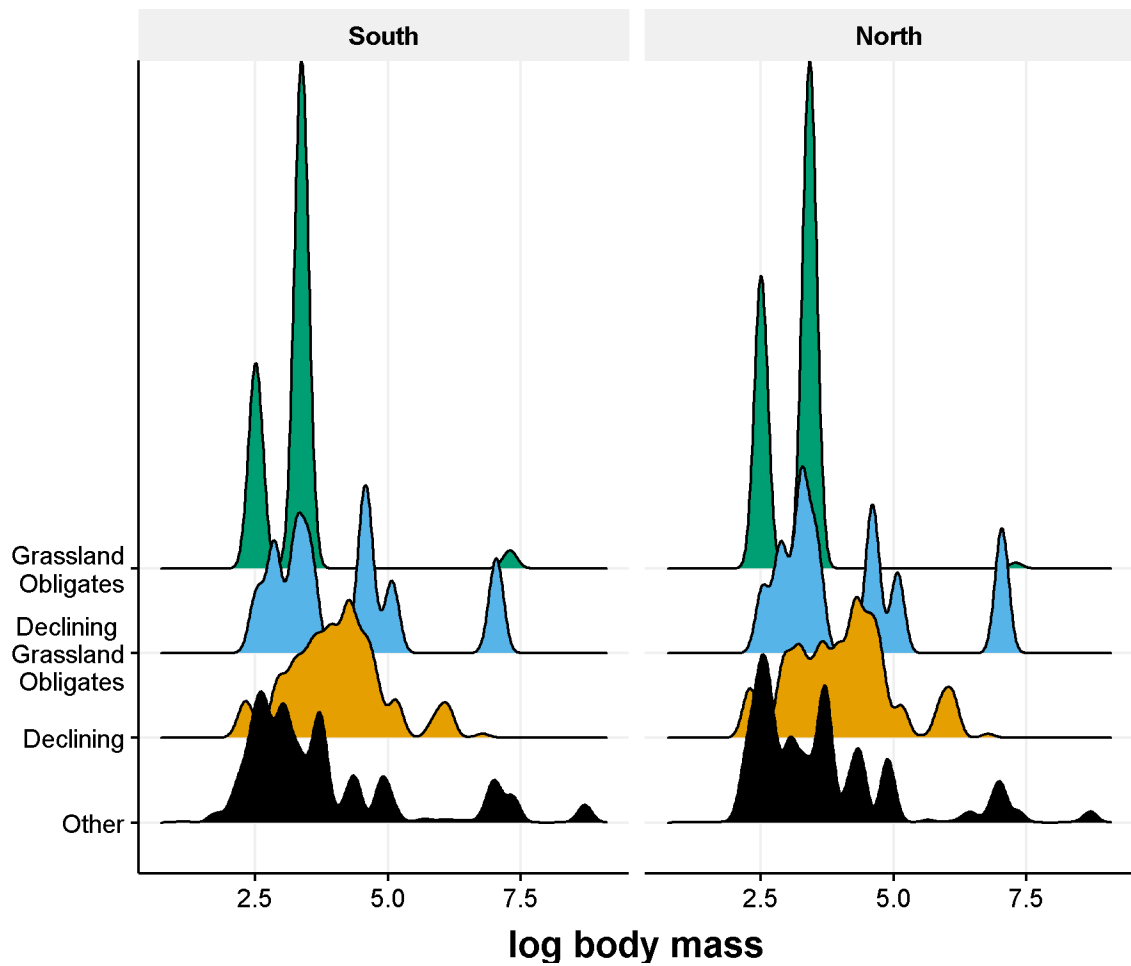


Figure 11: The body mass distribution of declining species appears to differ slightly between the Southern and Northern regimes.

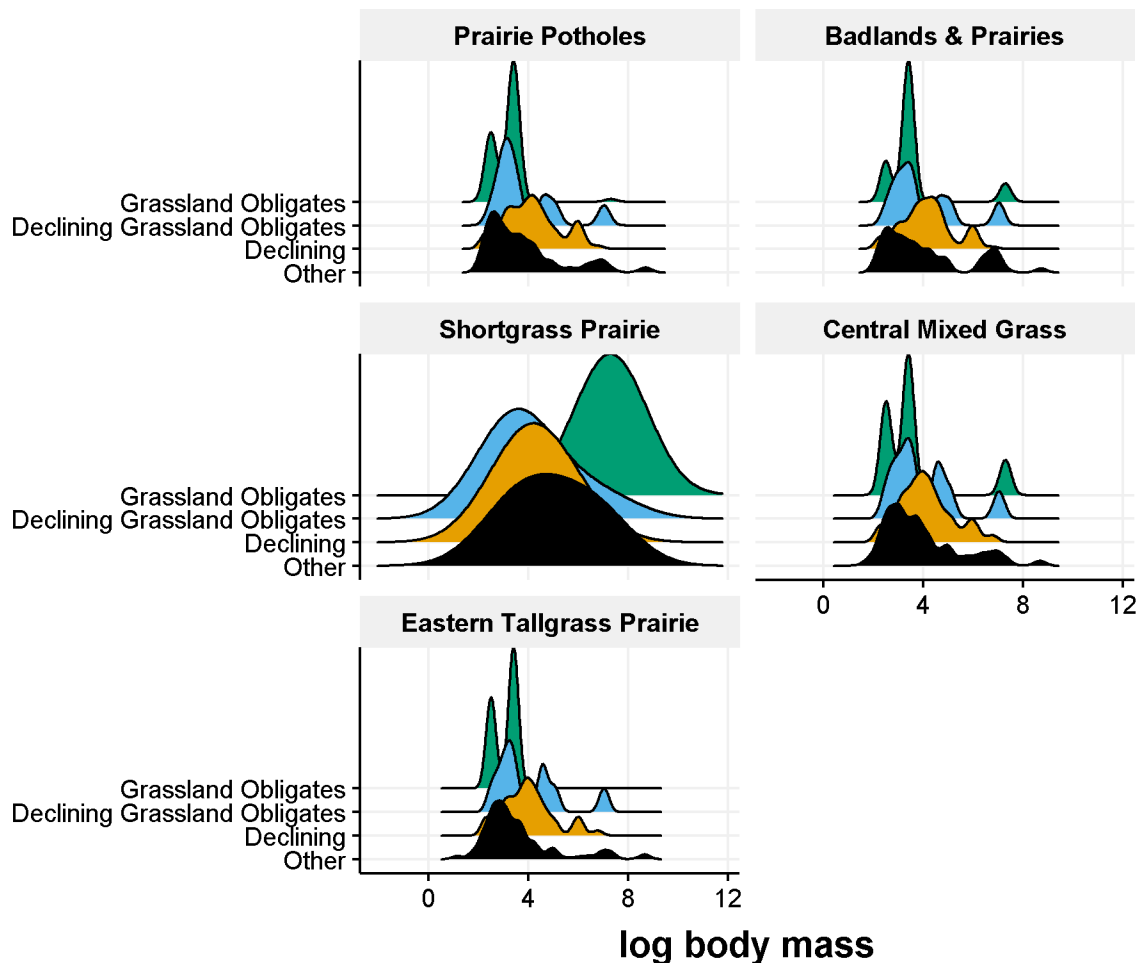
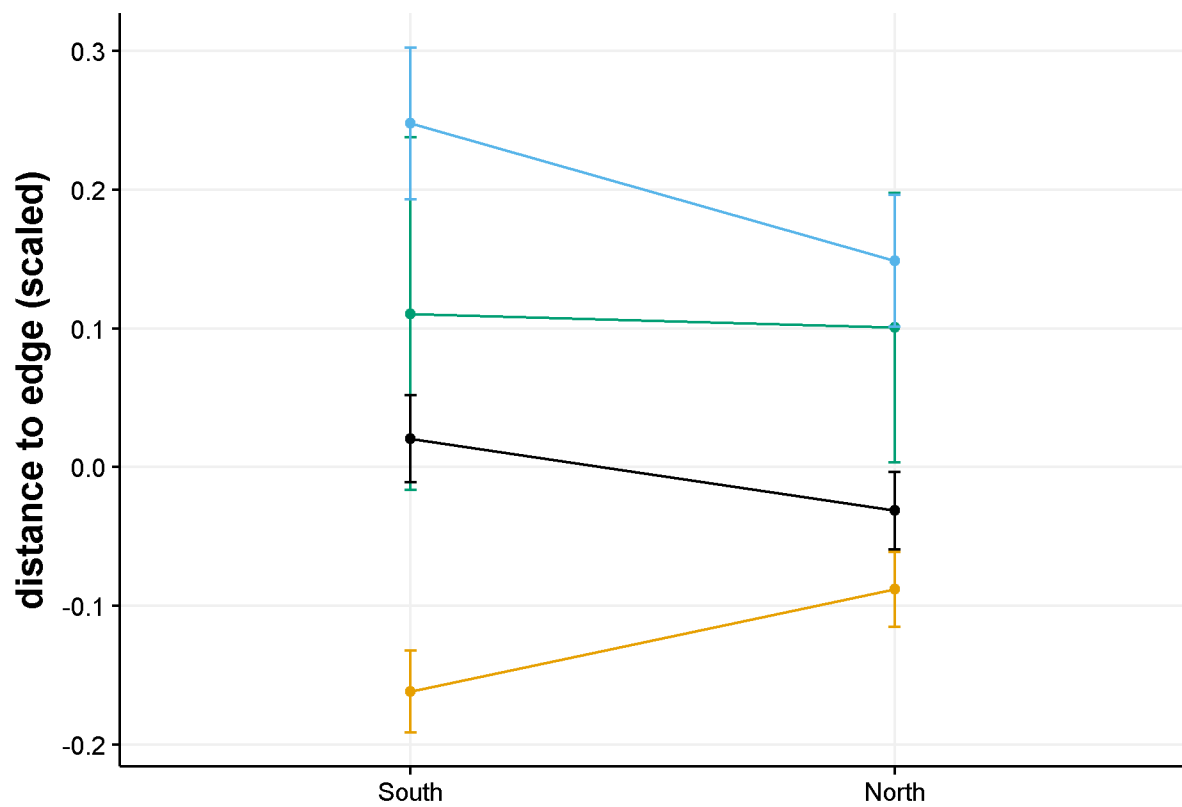
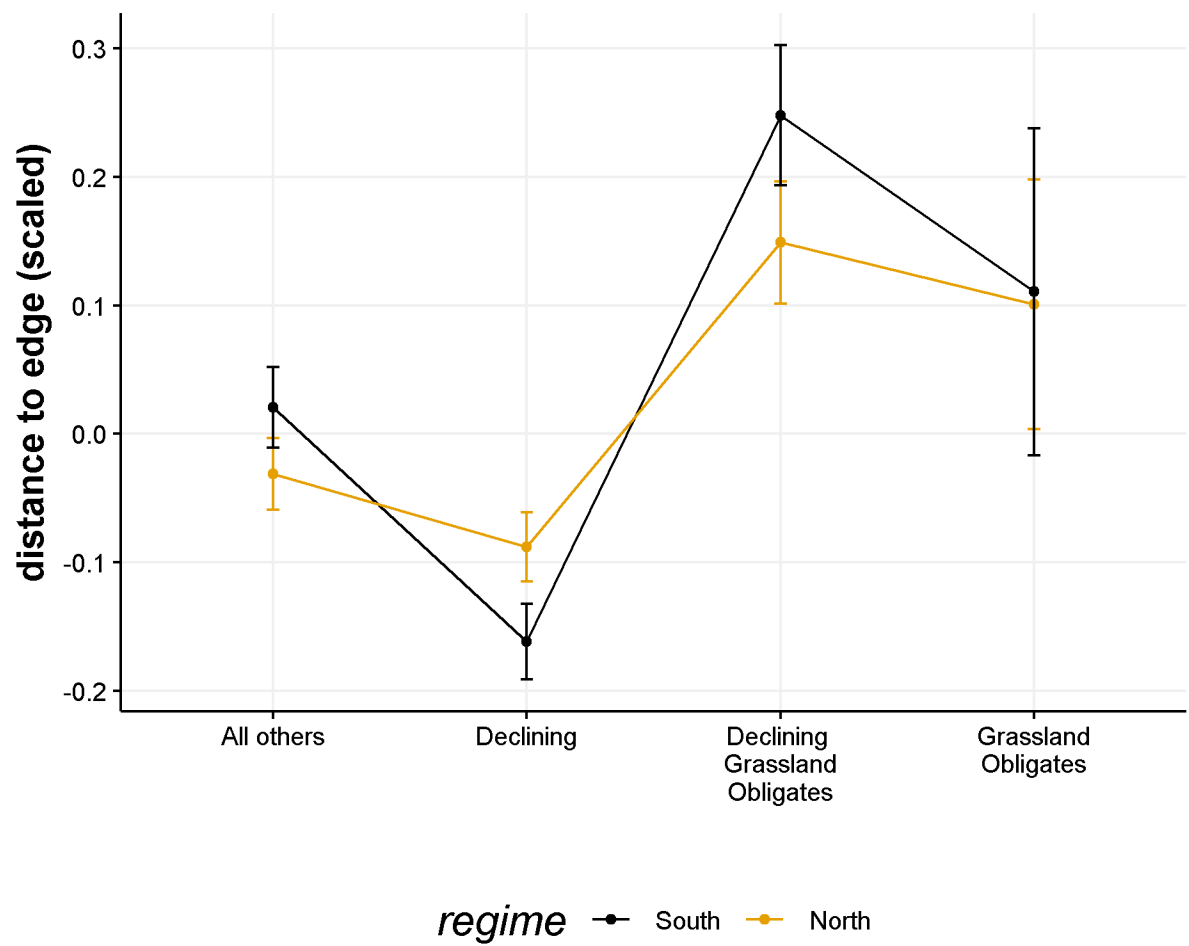


Figure 12: Body mass distribution for species in the study area over the entire time period varies by species group. Distributions represent the species pool for each group and Bird Conservation Region over all years.



sppGroup ● allOthers ● declining ● grassDeclining ● grassObli



the findings of these methods, however, is in its infancy. In this Chapter, I used discontinuity analysis of bird communities, under the assumption of a zone of shifting ‘spatial regimes’ [roberts2019shifting] to determine whether local-scale changes in the scaling structure were impacted by these shifts. Although I found moderate support for the hypothesis that declining species operate at the edges of body mass aggregations, I did not find sufficient support for the impact of these proposed spatial regime shifts.

Although the body mass distributions of terrestrial communities at small scales tends to differ from the distribution at larger spatial scales [blackburn1994animal], numerous studies confirm the evidence for ‘discontinuities’ in these distributions at across scales for a variety of phenomenon [wardwell2009variability; allen199body; spanbauer2016body; nash2014discontinuities]. The jury is still out, however, as numerous studies are finding a lack of evidence for discontinuities in their study systems [siemann1999gaps; bibi2019body; manly1996there].

Table 1: Grassland obligates and species with declining trends over the period of (1966-2015) in the Central Breeding Bird Survey region in our study area.

Common Name	Species Group
Bobolink	Grassland Obligates
Lark Sparrow	Grassland Obligates
Chipping Sparrow	Grassland Obligates
Henslow's Sparrow	Grassland Obligates
Ferruginous Hawk	Grassland Obligates
Upland Sandpiper	Declining Grassland Obligates
Ring-necked Pheasant	Declining Grassland Obligates
Horned Lark	Declining Grassland Obligates
Eastern Meadowlark	Declining Grassland Obligates
Western Meadowlark	Declining Grassland Obligates
Vesper Sparrow	Declining Grassland Obligates
Grasshopper Sparrow	Declining Grassland Obligates
Field Sparrow	Declining Grassland Obligates
Dickcissel	Declining Grassland Obligates
Savannah Sparrow	Declining Grassland Obligates
Lark Bunting	Declining Grassland Obligates
Cassin's Sparrow	Declining Grassland Obligates
Chestnut-collared Longspur	Declining Grassland Obligates
Killdeer	Declining
Northern Bobwhite	Declining
Rock Pigeon	Declining
Mourning Dove	Declining
Yellow-billed Cuckoo	Declining
Black-billed Cuckoo	Declining
Belted Kingfisher	Declining
Downy Woodpecker	Declining
Red-headed Woodpecker	Declining
Red-bellied Woodpecker	Declining
Chimney Swift	Declining
Eastern Kingbird	Declining
Western Kingbird	Declining
Great Crested Flycatcher	Declining
Blue Jay	Declining
American Crow	Declining
European Starling	Declining
Red-winged Blackbird	Declining
Orchard Oriole	Declining
Baltimore Oriole	Declining
Common Grackle	Declining
Song Sparrow	Declining
Purple Martin	Declining
Barn Swallow	Declining
Loggerhead Shrike	Declining
Common Yellowthroat	Declining
House Sparrow	Declining
Brown Thrasher	Declining
Black-capped Chickadee	Declining
Gray Partridge	Declining
Wood Thrush	Declining
Northern Harrier	Declining
Greater Prairie-Chicken	Declining
Scissor-tailed Flycatcher	Declining

Table 2: The number of NABBS routes analysed in the Southern regime is smaller than those used in the Northern regime each year given the location of the regimes identified in a previous study with respect to the contiguous grasslands of Central North America (see Figure ref(fig:studyarea)).

Year	North	South
1967	38	11
1968	43	12
1969	53	11
1970	45	17
1971	43	13
1972	38	17
1973	39	15
1974	29	17
1975	41	16
1976	46	18
1977	47	16
1978	45	18
1979	46	17
1980	43	16
1981	40	18
1982	38	16
1983	37	16
1984	30	14
1985	30	24
1986	31	21
1987	36	21
1988	34	24
1989	33	25
1990	40	21
1991	31	22
1992	33	23
1993	39	23
1994	37	23
1995	37	22
1996	39	22
1997	36	24
1998	34	21
1999	32	23
2000	37	37
2001	31	34
2002	32	36
2003	36	38
2004	35	35
2005	38	36
2006	39	35
2007	39	36
2008	35	34
2009	39	37
2010	37	30
2011	38	33
2012	33	35
2013	39	37
2014	42	38
2015	36	33
2016	37	30
2017	35	32

Table 3: Summary statistics for annual species richness and annual turnover in all NABBS routes in study area.

Year	Annual Richness			Annual Turnover		
	\bar{x}	σ	N	\bar{x}	σ	N
1967	39.4	8.14	27	-0.1	8.13	27
1968	41.4	8.11	37	1.6	10.25	37
1969	39.9	7.44	47	0.6	10.12	47
1970	41.3	7.73	43	0.9	9.74	43
1971	39.4	7.50	36	0.7	10.62	36
1972	41.0	9.80	32	-1.2	12.94	32
1973	40.1	8.33	33	-2.1	10.42	33
1974	38.8	7.67	27	-2.2	10.53	27
1975	38.3	7.37	32	-1.4	9.57	32
1976	41.2	7.53	45	0.6	10.31	45
1977	39.5	8.48	43	-1.7	9.69	43
1978	39.5	8.88	42	-1.9	10.09	42
1979	39.7	8.06	43	-1.7	10.03	43
1980	40.4	7.18	37	-1.1	10.16	37
1981	41.2	8.76	39	-1.2	9.26	39
1982	42.3	6.65	32	-1.6	8.28	32
1983	41.3	8.47	33	-1.9	8.91	33
1984	41.7	7.85	22	-4.1	6.12	22
1985	40.8	8.54	34	-1.1	11.30	34
1986	42.2	9.17	32	-2.7	10.42	32
1987	43.4	8.94	38	-1.3	9.82	38
1988	41.7	9.35	37	-1.4	12.19	37
1989	42.3	8.67	40	-1.8	9.98	40
1990	42.3	9.47	38	-1.6	9.69	38
1991	43.3	9.69	30	-2.1	10.14	30
1992	44.6	7.52	31	-0.8	9.61	31
1993	42.7	9.35	41	-1.0	12.87	41
1994	43.4	9.76	38	0.4	12.50	38
1995	42.2	9.98	39	-0.8	12.75	39
1996	44.1	7.44	36	1.0	10.68	36
1997	44.6	9.45	39	1.0	12.65	39
1998	43.8	9.00	32	-1.9	12.25	32
1999	45.9	9.52	28	-1.8	11.66	28
2000	45.8	9.30	56	0.5	11.86	56
2001	46.5	8.51	46	0.7	11.95	46
2002	46.8	8.94	50	0.5	13.91	50
2003	48.1	9.84	57	-0.2	13.11	57
2004	45.8	10.88	49	0.1	13.97	49
2005	46.3	9.13	52	-0.6	11.20	52
2006	46.2	10.46	52	-0.5	11.94	52
2007	46.7	9.59	57	0.3	11.29	57
2008	48.2	11.00	47	1.0	14.84	47
2009	47.8	9.92	56	-0.4	12.11	56
2010	47.4	9.62	45	-0.9	11.93	45
2011	47.0	10.53	47	-1.0	14.61	47
2012	47.7	10.33	46	0.7	13.46	46
2013	47.0	10.03	57	1.1	13.50	57
2014	47.8	9.35	59	-0.2	11.22	59
2015	48.5	9.33	49	0.4	10.79	49
2016	50.8	9.38	44	2.0	12.73	44
2017	47.6	9.84	45	0.2	11.84	45